

The Q^2 dependence of the measured asymmetry A_1 from the similarity of $g_1(x, Q^2)$ and $F_3(x, Q^2)$ structure functions

A.V.Kotikov ¹ and D.V.Peshekhonov ²

*Particle Physics Laboratory
Joint Institute for Nuclear Research
141980 Dubna, Russia.*

Abstract

We propose a new approach for taking into account the Q^2 dependence of measured asymmetry A_1 . This approach is based on the similarity of the Q^2 behaviour and the shape of the spin-dependent structure function $g_1(x, Q^2)$ and spin averaged structure function $F_3(x, Q^2)$. The analysis is applied on available experimental data.

PACS number(s): 13.60.Hb, 11.55.Hx, 13.88.+e

¹ E-mail: kotikov@sunse.jinr.ru; Anatoli.Kotikov@cern.ch

² E-mail: Dimitri.Pechekhonorov@inf.n.trieste.it; Dimitri.Pechekhonorov@cern.ch
presently at INFN sezione di Trieste, Italia

1 Introduction

In a recent years there has been a significant progress in the study of the spin-dependent structure function (SF) $g_1(x, Q^2)$ (see [1]-[6]). The direct measurement of SF g_1 is very elaborate procedure (see, however, [7]) and ordinary its value is extracted from the spin dependent asymmetry A_1 (see, for example [8, 9]) in agreement with the following formula:

$$g_1(x, Q^2) = A_1(x, Q^2) \cdot F_1(x, Q^2), \quad (1)$$

where $F_1(x, Q^2)$ is the spin average SF.

The asymmetry $A_1(x, Q^2)$ is closely connected with the ratio of polarized and unpolarized cross-sections and may be "easy" measured due to cancelation of many experimental uncertainties. Experimentally asymmetry is extracting only at few points $Q_{1i}^2, \dots, Q_{ni}^2$ for each x_i bin. To study the properties of $g_1(x, Q^2)$ and to calculate the values of spin dependent sum rules [10, 11] we have to know the A_1 as a function of Q^2 .

The most popular assumption applied on A_1 [12] is

$$A_1(x, Q^2) = A_1(x), \quad (2)$$

It means that SF g_1 and F_1 have the same Q^2 dependences what does not following from the theory. On the contrary, the behaviour of F_1 and g_1 as a functions of Q^2 is expected to be different due to the difference between polarized and unpolarized splitting functions³.

There are several approaches [13]-[18] how to take into account the Q^2 dependence of A_1 . They are based on the different approximate solutions of the DGLAP equations. Some of them have been used already by Spin Muon Collaboration (SMC) and E154 Collaboration in the last analyses of experimental data (see [2] and [6], respectively). These approaches [13]-[18] lead to similar results in $g_1(x, Q^2)$ ⁴ which are contrast with the calculations based on Eq.(2).

In this article we suggest another method how to take into account Q^2 dependence of A_1 which is based on the observation that the splitting functions of the DGLAP equations for the SF g_1 and F_3 and the shapes of these SF are similar in a wide x range. Our approach allows to set Q^2 -dependence of A_1 in a very simple way (see Eq.(10)) and leads to the results (some of them have been recently presented [19] on the Workshop DIS98), which are similar with ones based on the DGLAP evolution.

2 The Q^2 dependence of structure functions

Lets consider the Q^2 evolution of nonsinglet (NS) and singlet (SI) parts of the SF separately.

For the SF F_3 and the nonsinglet (NS) parts of g_1 and F_1 the corresponding DGLAP equations can be presented as⁵ as:

³except the leading order of the quark-quark interaction.

⁴ The form of the Q^2 -dependence for A_1 is different in approaches [13]-[18]. However, all of them are in agreement with the weak Q^2 -dependence at moderate x and quite strong at small x region.

⁵We use $\alpha(Q^2) = \alpha_s(Q^2)/4\pi$.

$$\begin{aligned}
\frac{dg_1^{NS}(x, Q^2)}{d\ln Q^2} &= -\frac{1}{2}\gamma_{NS}^-(x, \alpha) \otimes g_1^{NS}(x, Q^2), \\
\frac{dF_1^{NS}(x, Q^2)}{d\ln Q^2} &= -\frac{1}{2}\gamma_{NS}^+(x, \alpha) \otimes F_1^{NS}(x, Q^2), \\
\frac{dF_3(x, Q^2)}{d\ln Q^2} &= -\frac{1}{2}\gamma_{NS}^-(x, \alpha) \otimes F_3(x, Q^2),
\end{aligned} \tag{3}$$

where the symbol \otimes means the Mellin convolution:

$$f_1(x) \otimes f_2(x) \equiv \int_x^1 \frac{dz}{z} f_1(z) f_2\left(\frac{x}{z}\right)$$

The splitting functions $\gamma_{NS}^\pm(x, \alpha)$ are the reverse Mellin transforms of the anomalous dimensions $\gamma_{NS}^\pm(n, \alpha) = \alpha\gamma_{NS}^{(0)}(n) + \alpha^2\gamma_{NS}^{\pm(1)}(n) + O(\alpha^3)$ and the Wilson coefficients⁶ $\alpha b^\pm(n) + O(\alpha^2)$:

$$\gamma_{NS}^\pm(x, \alpha) = \alpha\gamma_{NS}^{(0)}(x) + \alpha^2\left(\gamma_{NS}^{\pm(1)}(x) + 2\beta_0 b^\pm(x)\right) + O(\alpha^3), \tag{4}$$

where $\beta(\alpha) = -\alpha^2\beta_0 - \alpha^3\beta_1 + O(\alpha^4)$ is QCD β -function.

Eqs. (3) show that the DGLAP equations for F_3 and for the NS part of g_1 are the same (it was obtained exactly in first two orders of the perturbative QCD⁷ [20]) and differ from the one for F_1 already in the first subleading order ($\gamma_{NS}^{+(1)} \neq \gamma_{NS}^{-(1)}$ [21] and $b_{NS}^+ - b_{NS}^- = (8/3)x(1-x)$).

For the SI parts of g_1 and F_1 evolution equations are :

$$\begin{aligned}
\frac{dg_1^S(x, Q^2)}{d\ln Q^2} &= -\frac{1}{2}\left[\gamma_{SS}^*(x, \alpha) \otimes g_1^S(x, Q^2) + \gamma_{SG}^*(x, \alpha) \otimes \Delta G(x, Q^2)\right], \\
\frac{dF_1^S(x, Q^2)}{d\ln Q^2} &= -\frac{1}{2}\left[\gamma_{SS}(x, \alpha) \otimes F_1^S(x, Q^2) + \gamma_{SG}(x, \alpha) \otimes G(x, Q^2)\right],
\end{aligned} \tag{5}$$

where the SI splitting functions $\gamma_{Si}(x, \alpha)$ ($i = \{S, G\}$) are represented as

$$\begin{aligned}
\gamma_{SS}(x, \alpha) &= \alpha\gamma_{SS}^{(0)}(x) + \alpha^2\left(\gamma_{SS}^{(1)}(x) + b_G(x) \otimes \gamma_{GS}^{(0)}(x) + 2\beta_0 b_S(x)\right) + O(\alpha^3), \\
\gamma_{SG}(x, \alpha) &= \frac{e}{f}\left[\alpha\gamma_{SG}^{(0)}(x) + \alpha^2\left(\gamma_{SG}^{(1)}(x) + b_G(x) \otimes (\gamma_{GG}^{(0)}(x) - \gamma_{SS}^{(0)}(x)) + 2\beta_0 b_G(x) \right. \right. \\
&\quad \left. \left. + b_S(x) \otimes \gamma_{SG}^{(0)}(x)\right)\right] + O(\alpha^3)
\end{aligned} \tag{6}$$

and $e = \sum_i^f e_i^2$ is the sum of charge squares of f active quarks. Equations for the polarized singlet splitting functions $\gamma_{SS}^*(x, \alpha)$ and $\gamma_{SG}^*(x, \alpha)$ are similar. They can be obtained from

⁶We consider here structure functions but not the parton distributions. Note also that $b_{NS}^+(n)$ and $b_{NS}^-(n)$ can be defined as $b_{1,NS}(n) = b_{2,NS}(n) - b_{L,NS}(n)$ and $b_{3,NS}(n)$.

⁷It is easy to demonstrate in any order of perturbation theory. The SF g_1 and F_3 are the results of the γ_5 matrix contribution to the lepton and hadron parts of deep-inelastic cross-sections, respectively. In the NS case there is only one γ -matrix trace, connecting the lepton and hadron parts. Its contribution $\sim \text{tr}(\gamma_5 \gamma_\mu \gamma_\nu \gamma_\alpha \gamma_\beta \dots)$ is the same in both cases above. For the SI part of g_1 there are diagrams with several traces, which arise in the second order of perturbation QCD and lead to the difference between the splitting functions of SF F_3 and the SI part of SF g_1 .

(6) by replacing $\gamma_{SG}^{(0)}(x) \rightarrow \gamma_{SG}^{*(0)}(x)$, $\gamma_{Si}^{(1)}(x) \rightarrow \gamma_{Si}^{*(1)}(x)$ and $b_i(x) \rightarrow b_i^*(x)$ ($i = \{S, G\}$).

Careful consideration of the quark part of (5) and (6) shows that the value $b_s^*(x)$ ($b_s(x)$) coincides with $b^-(x)$ ($b^+(x)$). The difference between $\gamma_{NS}^{-(1)}(x)$ and $\gamma_{SS}^{*(1)}(x) + b_G^*(x) \otimes \gamma_{GS}^{(0)}(x)$ is negligible because it does not contain a power singularity at $x \rightarrow 0$ (i.e. a singularity at $n \rightarrow 1$ in momentum space). Moreover, this difference decreases as $O(1-x)$ at $x \rightarrow 1$ [24] (contrary to this, the difference between $\gamma_{SS}^{(1)}(x) + b_G(x) \otimes \gamma_{GS}^{(0)}(x)$ and $\gamma_{SS}^{*(1)}(x) + b_G^*(x) \otimes \gamma_{GS}^{(0)}(x)$ contains the power singularity at $x \rightarrow 0$ (see for example [20])). Thus, the DGLAP equations for F_3 and the SI part of g_1 have a close splitting functions, which are essentially different from the splitting functions of the SI part of F_1 .

The quark part of SI SF g_1 itself contains two components: valence and sea. Valence part does not connect with the gluon and obeys the DGLAP equation similar to first equation of (3). The sea part obeys the first equation of (5). This contribution was not observed experimentally yet.

The contribution of the gluon distribution in g_1 is not so important for the modern data (see [14, 15, 9, 18, 22]) (in a contrary to unpolarized case): data are described well for extremally different values of $\Delta G(x, Q^2)$ and even for different sign. Hence we will neglect this term in our analysis.

Thus, the valence component seems to dominate in SI part of g_1 at the range of the present experimental data⁸ and it allows us to expect a similarity of SI part of g_1 and SF F_3 .

As we saw from above, the shapes and DGLAP equations for g_1 and F_3 are very close in NS and SI analyses⁹ and both of them differ from the corresponding equations for F_1 . This similarity leads to close Q^2 dependence of SF $g_1(x, Q^2)$ and $F_3(x, Q^2)$.

The similarity of Q^2 dependence of $F_3(x, Q^2)$ and $g_1(x, Q^2)$ may be also supported by some arguments following from analysis at $x \rightarrow 0$ ¹⁰. Although all existed data in polarized DIS (exclude two first SMC points) are outside from the region $x \leq 10^{-2}$, the study of small x asymptotics is important as for the future data, as for an extrapolation of the present data to the small x region.

The similarity of the splitting functions of SF F_3 and g_1 have been already demonstrated and, thus, we have to discuss now the shapes of F_3 and g_1 at small x . It is well known that SF F_3 is governed at small x by ρ -meson trajectory and, thus,

$$F_3(x) \sim x^{-1/2} \quad (7)$$

The Q^2 -evolution does not change this behaviour. For SF g_1 the situation is not so clear. From Regge analysis [26] the NS part of g_1 is governed by a_1 trajectory, i.e. $g_1(x) \sim x^{-\alpha_P(a_1)}$ with the intercept $\alpha_P(a_1)$ having values $0 \geq \alpha_P(a_1) \geq -1/2$ (see [27]). However, the BFKL inspired approach [28] leads to more singular behaviour for NS part:

$$g_1^{NS}(x) \sim x^{-0.45}, \quad (8)$$

⁸To support of this point of view, one can see also the recent analysis of E154 Collaboration [6], where the contribution of sea + gluon and valence parts are divided, studied and presented in Fig. 2 of [6].

⁹The similar shapes of SF F_3 and g_1 in the range of measured values of x one can see also in the analysis [25].

¹⁰At $x \rightarrow 1$ the behaviour of g_1 and F_3 (and F_1 , too) should be similar because it is governed by valence quark distributions.

which is close to (7). For SI part of g_1 an information is very poor. The BFKL inspired approach [29] leads to the small x behaviour $g_1^{SI}(x) \sim x^{-1}$, but really SI part of g_1^{11} was not observed at small x yet. It is also connected with the fact that the deuteron SF $g_1^d(x)$, which is close to the SI component, is comparable with zero at small x .

As a consequences, the shapes of SF F_3 and the NS part of SF g_1 seems to be close also at small x (if BFKL approach is correct at least). The SI part of g_1 may has another shape but modern experimental data do not allow to study it.

The analysis discussed above allows us to conclude that the function A_1^* defined as:

$$A_1^*(x) = \frac{g_1(x, Q^2)}{F_3(x, Q^2)} \quad (9)$$

has to be practically Q^2 independent in the hole region of modern experimental data [1]-[6].

In agreement with Eq.(9) measured asymmetry $A_1(x_i, Q_i^2)$ can be found at some value of Q^2 as:

$$A_1(x_i, Q^2) = \frac{F_3(x_i, Q^2)}{F_3(x_i, Q_i^2)} \cdot \frac{F_1(x_i, Q_i^2)}{F_1(x_i, Q^2)} \cdot A_1(x_i, Q_i^2) \quad (10)$$

3 Calculation of $A_1(x, Q^2)$ and $\Gamma_1(Q^2)$.

To apply this approach we used¹² the SMC [2], E143 [4] and E154 [5, 6] collaboration data. To use relation (10) we have parametrized CCFR data on $F_2(x, Q^2)$ and $xF_3(x, Q^2)$ [30] in the form the same with NMC fit of the structure function $F_2(x, Q^2)$ [31] (see Appendix). To obtain structure function $F_1(x, Q^2)$ we take the parametrization of the CCFR data on $F_2(x, Q^2)$ [30] and SLAC parametrization of $R(x, Q^2)$ [32] and use relation :

$$F_1(x, Q^2) = \frac{F_2(x, Q^2)}{2x(1 + R(x, Q^2))} \cdot (1 + \frac{4M^2x^2}{Q^2}), \quad (11)$$

where M is the proton mass.

The fact that we use in Eq.(10) parametrizations of CCFR data [30] for both SF $xF_3(x, Q^2)$ and $F_2(x, Q^2)$ allows to avoid systematical uncertainties and nucleon correlation in nuclei.

Fig. 1 shows the ratio $A_1(Q^2)/A_1(5GeV^2)$ obtained with Eq.(10). Comparison of Fig. 1 with the results of E154 Collaboration (Fig. 4 in [6]) shows quite good agreement.

The SF $g_1(x, Q^2)$ was evaluated using Eq.(1) where spin average SF F_1 has been calculated using NMC parametrization of $F_2(x, Q^2)$ [31]. Results are presented in Fig. 2 and Fig. 3 for E154 and SMC data, respectively. Our results are in excellent agreement with the SMC and E154 Collaboration analyses based on direct DGLAP evolution (see [2] and [6], respectively).

To make a comparison with the theory predictions on the sum rules we have calculated also the first moment value of the structure function g_1 at different Q^2

$$\Gamma_1 = \tilde{\Gamma}_1 + \Delta\tilde{\Gamma}_1, \quad (12)$$

¹¹Correctly, sea component of SI part of g_1 , which dominates here if it has nonzero magnitude.

¹²Similar analysis of SMC data of [1] has been done in [33] using old CCFR data [35].

where

$$\tilde{\Gamma}_1(Q^2) = \int_{x_{min}}^{x_{max}} g_1(x, Q^2) dx \quad \text{and} \quad \Delta\tilde{\Gamma}_1(Q^2) = \int_0^{x_{min}} g_1(x, Q^2) dx + \int_{x_{max}}^1 g_1(x, Q^2) dx \quad (13)$$

are the integral through the measured kinematical x region plus an estimation for unmeasured ranges, respectively.

The value of $\Delta\tilde{\Gamma}_1$ coming from the unmeasured x -regions was estimated using original methodics by “owner-collaborations”. We have to note here that the methodic of $\Delta\tilde{\Gamma}_1$ estimation may leads to some underestimation of $g_1^{p,d,n}(x, Q^2)$ at small x and of $\Gamma^{p,d,n}(Q^2)$, as a consequence (see the careful analysis in [14]). To clear up this situation it is necessary to have more precise data at small x .

Values of $\Gamma_1(Q^2)$ which are obtained from the exact solution of the DGLAP evolution equation [2, 6] of $g_1(x, Q^2)$ and A_1 [1]-[6] and in our approach on the scaling of A_1^* are quite close each other for all cases discussed here. Thus all approaches lead to the similar conclusions on $\Gamma^{p,d,n}(Q^2)$ and the results are in a strong disagreement with the theoretical predictions [36], we will consider the effect of A_1^* scaling only for the Bjorken Sum rule $\Gamma_1^p - \Gamma_1^n$.

Deuteron SMC and E143 data allow us to extract the value of Γ_1^n :

$$\Gamma_1^p + \Gamma_1^n = \frac{2\Gamma_1^d}{1 - 1.5w_d}, \quad (14)$$

where $w_d=0.05$ is the the probability of the deuteron to be in a D-state. Knowledge of proton and neutron first momenta $\Gamma_1^{p,n}$ allows to test the Bjorken sum rule:

$$\Gamma_1^{p-n} \equiv \int_0^1 (g_1^p(x, Q^2) - g_1^n(x, Q^2)) dx = \Gamma_1^p - \Gamma_1^n \quad (15)$$

Results are presented in the Table 1 in comparison with values published by SMC, E143 and E154 Colaborations and with the theoretical predictions computed in the third order in the QCD α_s [37].

Let us now describe the main results, which follow from the Table 1 and the Figures.

- Our description of the Q^2 evolution of the asymmetry $A_1(x, Q^2)$ has very simple form (10) but gives results which are in good agreement with a powerfull analyses [14, 15, 6].
- Results on $g_1(x, Q^2)$ are in excelent agreement with SMC and E154 Collaborations analyses, based on direct DGLAP evolution.
- Our method allows to test sum rules in a simple way with a good accuracy. Obtained results on the $\Gamma_1^p - \Gamma_1^n$ show that used experimental data well confirm the Bjorken sum rule prediction.

4 Conclusion

We have considered the Q^2 evolution of the asymmetry $A_1(x, Q^2)$ based on the similarity of Q^2 dependence of the SF $g_1(x, Q^2)$ and $F_3(x, Q^2)$ ¹³. Obtained results on $g_1(x, Q^2)$ are in

¹³The usefull parametrizations of SF $F_2(x, Q^2)$ and $xF_3(x, Q^2)$ are obtained for new CCFR data and presented in Appendix.

excellent agreement with the corresponding results of SMC and E154 Collaborations, based on direct DGLAP evolution. Our test of the Ellis-Jaffe sum rules for the proton, deuteron and neutron are very close to the values published by Spin Muon, E143 and E154 Collaborations. However, the corrections coming due to Q^2 evolution of asymmetry $A_1(x, Q^2)$ have an opposite signs for the proton and deuteron. It leads to the improvement in agreement between the experiment and the theoretical prediction on the Bjorken sum.

We believe that future precise data will illuminate a violation of our hypothese (probably, at very small x values: $x \leq 10^{-3}$). This violation will indicate clearly the appearance of nonzero contributions from sea quark and gluon components of SF $g_1(x, Q^2)$ having quite singular shapes at small x ¹⁴ (see the carefull analysis in [38]). Thus, check of the Q^2 -dependence of the ratio $A_1^* = g_1/F_3$ for a future precise data leads to make a qualitative estimations shapes and Q^2 -dependences of gluon and sea quark distributions.

Acknowledgements

We are grateful to W.G. Seligman for providing us the available CCFR data of Refs.[30, 35], to A.V. Efremov and O.V. Teryaev for interest to this work and discussions and to A.P. Nagaitsev for a collaboration in the beginning of this study.

Appendix

The parametrizations are used for CCFR data [35] :

$$xF_3(x, Q^2) = F_3^a \cdot \left(\frac{\log(Q^2/\Lambda^2)}{\log(Q_0^2/\Lambda^2)} \right)^{F_3^b} \quad \text{and} \quad F_2(x, Q^2) = F_2^a \cdot \left(\frac{\log(Q^2/\Lambda^2)}{\log(Q_0^2/\Lambda^2)} \right)^{F_2^b},$$

where

$$F_3^a = x^{C_1} \cdot (1-x)^{C_2} \cdot \left(C_3 + C_4 \cdot (1-x) + C_5 \cdot (1-x)^2 + C_6 \cdot (1-x)^3 + C_7 \cdot (1-x)^4 \right)$$

$$F_2^a = x^{B_1} \cdot (1-x)^{B_2} \cdot \left(B_3 + B_4 \cdot (1-x) + B_5 \cdot (1-x)^2 + B_6 \cdot (1-x)^3 + B_7 \cdot (1-x)^4 \right)$$

$$F_3^b = C_8 + C_9 \cdot x + \frac{C_{10}}{x + C_{11}} \quad \text{and} \quad F_2^b = B_8 + B_9 \cdot x + \frac{B_{10}}{x + B_{11}}$$

and $Q_0^2 = 20 \text{ GeV}^2$, $\Lambda = 337 \text{ MeV}$. The values of Q_0^2 and Λ are fixed in agreement with CCFR analysis [30]. The values of the coefficients C_i ($i = 1, \dots, 11$) and B_i ($i = 1, \dots, 15$) are given in Table 2.

¹⁴In the case of a similar shapes of SI and NS components the separation and study of them will be quite elaborate procedure.

References

- [1] SMC, D. Adams, *et al.*, Phys. Lett. B **329**, 399 (1994), B **339**, 332(E) (1994), Phys. Lett. B **357**, 248 (1995); E143 Collab., K. Abe, *et al.*, Phys. Rev. Lett. **74**, 346 (1995), Phys. Rev. Lett. **75**, 25 (1995); HERMES Collab., K. Ackerstaff, *et al.*, Phys. Lett. B **404**, 383 (1997).
- [2] SMC, D. Adams, *et al.*, Phys. Rev. D **56**, 5330 (1997).
- [3] SMC, D. Adams, *et al.*, Phys. Lett. B **396**, 338 (1997).
- [4] E143 Collab., K. Abe, *et al.*, SLAC-PUB-7753 (hep-ph/9802357), Phys. Rev. D (in press).
- [5] E154 Collab., K. Abe, *et al.*, Phys. Rev. Lett. **79**, 26 (1997).
- [6] E154 Collab., K. Abe, *et al.*, Phys. Lett. B **405**, 180 (1997).
- [7] N. Gagunashvili, *et al.*, NIM **412**, 146 (1998).
- [8] M. Anselmino, A. Efremov, E. Leader, Phys. Rep. **261** (1995) 1; J. Ellis, M. Karliner, CERN-TH.279/95 and TAUP-2297-95, 1995 (unpublished); B.L. Ioffe, in **Proceedings of Quarks-94**, Vladimir, p.14.
- [9] G.P. Ramsey, Prog. Part. Nucl. Phys. **39**, 599 (1997).
- [10] J.D. Bjorken, Phys. Rev. **148**, 1467 (1966); D **1**, 1376 (1970).
- [11] J. Ellis, R.L. Jaffe, Phys. Rev. D **9**, 1444 (1974); D **10**, 1669 (1974).
- [12] J. Ellis, M. Karliner, Phys. Lett. B **313**, 131 (1993); F.E. Close, R.G. Roberts, Phys. Lett. B **316**, 165 (1993).
- [13] G. Altarelli, P. Nason, G. Ridolfi, Phys. Lett. B **320**, 152 (1994); M. Gluck, E. Reya, W. Vogelsang, Phys. Lett. B **359**, 201 (1995); T. Gehrmann, W.J. Stirling, Z. Phys. C **65**, 470 (1995); E143 Collab., K. Abe, *et al.*, Phys. Lett. B **364**, 61 (1995); R.D. Ball, S. Forte, G. Ridolfi, Nucl. Phys. B **444**, 287 (1995); A.V. Kotikov, D.V. Peshekhonov, Phys. Rev. D **54**, 3162 (1996), Phys. of Atomic Nuclei, **60**, 653 (1997); T. Weigl, W. Melnitchouk, Nucl. Phys. B **465**, 267 (1996); G. Altarelli, *et al.*, Nucl. Phys. B **496**, 337 (1997); J.P. Nassalski, in **Proceeding of the XXVII International Conference on High Energy Physics (1996)** p. 35 (hep-ph/9612352).
- [14] M. Gluck, E. Reya, M. Stratmann, W. Vogelsang, Phys. Rev. D **53**, 4775 (1996).
- [15] T. Gehrmann, W.J. Stirling, Phys. Rev. D **53**, 6100 (1996).
- [16] R.D. Ball, S. Forte, G. Ridolfi, Phys. Lett. B **378**, 225 (1996).
- [17] M. Hirai, S. Kumano, M. Miyama, Comp. Phys. Commun. **108**, 38 (1998).
- [18] W.-D. Nowak, A.V. Sidorov, M.V. Tokarev, Nuovo Cim. A **110**, 757 (1997); E. Leader, A.V. Sidorov, D.B. Stamenov, hep-ph/9708335.
- [19] A.V. Kotikov, D.V. Peshekhonov, talk on **the Workshop DIS98** (hep-ph/9805374).

- [20] J. Kodaira, *et al.*, Phys. Rev. D **20**, 627 (1979); Nucl. Phys. B **159**, 99 (1979).
- [21] D.A. Ross, C.T. Sachrajda, Nucl. Phys. B **149**, 497 (1979); G. Altarelli, Phys. Rep. **81**, 1 (1982).
- [22] M. Goshtasbpour, G.P. Ramsey, Phys. Rev. D **55**, 1244 (1997); L. E. Gordon, M. Goshtasbpour, G.P. Ramsey, hep-ph/9803351.
- [23] FNAL E581/704 Collab., D.L. Adams, *et al.*, Phys. Lett. B **336**, 369 (1994).
- [24] R. Merting, W.L. van Neerven, Z. Phys. C **70**, 625 (1996); W. Vogelsang, Phys. Rev. D **54**, 2023 (1996).
- [25] C. Bourrely, J. Soffer, Nucl. Phys. B **445**, 341 (1995).
- [26] R.L. Heinmann, Nucl. Phys. B **64**, 429 (1973).
- [27] J. Ellis, M. Karliner, Phys. Lett. B **213**, 73 (1988).
- [28] J. Bartels, B.I. Ermolaev, M.G. Ryskin, Z. Phys. C **70**, 273 (1996).
- [29] J. Bartels, B.I. Ermolaev, M.G. Ryskin, Z. Phys. C **72**, 627 (1996).
- [30] CCFR/NuTeV Collab., W. Seligman, *et al.*, Phys. Rev. Lett. **79**, 1213 (1997); W. Seligman, Ph.D. thesis, Columbia University, Nevis Report 292, 1997.
- [31] NMC, M. Arneodo, *et al.*, Phys. Lett. B **364**, 107 (1995).
- [32] L.W. Whitlow, *et al.*, Phys. Lett. B **250**, 193 (1990).
- [33] A.V. Kotikov, D.V. Peshekhonov, JETP Lett. **65**, 7 (1997); in **Proceeding of the Workshop DIS96**, p.612 (hep-ph/9608369).
- [34] P. Ratchliffe, in **Proceeding of the International Symposium SPIN96**, p.161 (hep-ph/9611348).
- [35] CCFR Collab., P.Z. Quintas, *et al.*, Phys. Rev. Lett. **71**, 1307 (1993); M. Shaevitz, *et al.* Nucl. Phys. Proc. Suppl. B **38**, 188 (1995).
- [36] S.A. Larin, T. van Ritbergen, J.A.M. Vermaseren, Phys. Lett. B **404**, 153 (1997).
- [37] S.A. Larin, J.A.M. Vermaseren, Phys. Lett. B **259**, 345 (1991).
- [38] D. van Harrach, W.-D. Nowak, J. Soffer, Preprint DESY 97-232, CPT-97/P.3564, 1997 (hep-ph/9712207); A. De Roeck and T. Gehrmann, DESY 97-233, 1997 (hep-ph/9711512).

Figure Captions

Figure 1. Q^2 dependence of the ratio $A_1(x, Q^2)/A_1(x, 5GeV^2)$.

Figure 2. Structure function $xg_1^n(x, Q^2)$ evolved to $Q^2 = 5GeV^2$ using our eq.(10); DGLAP NLO evolution; the assumption that g_1^n/F_1^n is independent of Q^2 . Last two sets are taken from [6].

Figure 3. Structure function $xg_1^p(x, Q^2)$ evolved to $Q^2 = 10GeV^2$ using our eq.(10); the assumption that g_1^n/F_1^n is independent of Q^2 ; DGLAP NLO evolution according to the analyses of [13, 14]. Last two sets are taken from [2].

Table Captions

Table 1. The values of $\Gamma_1^p - \Gamma_1^n$. The errors are shown only for several points for each set of data. Uncertainties of our analysis are comparable with ones of [2, 3, 4, 6].

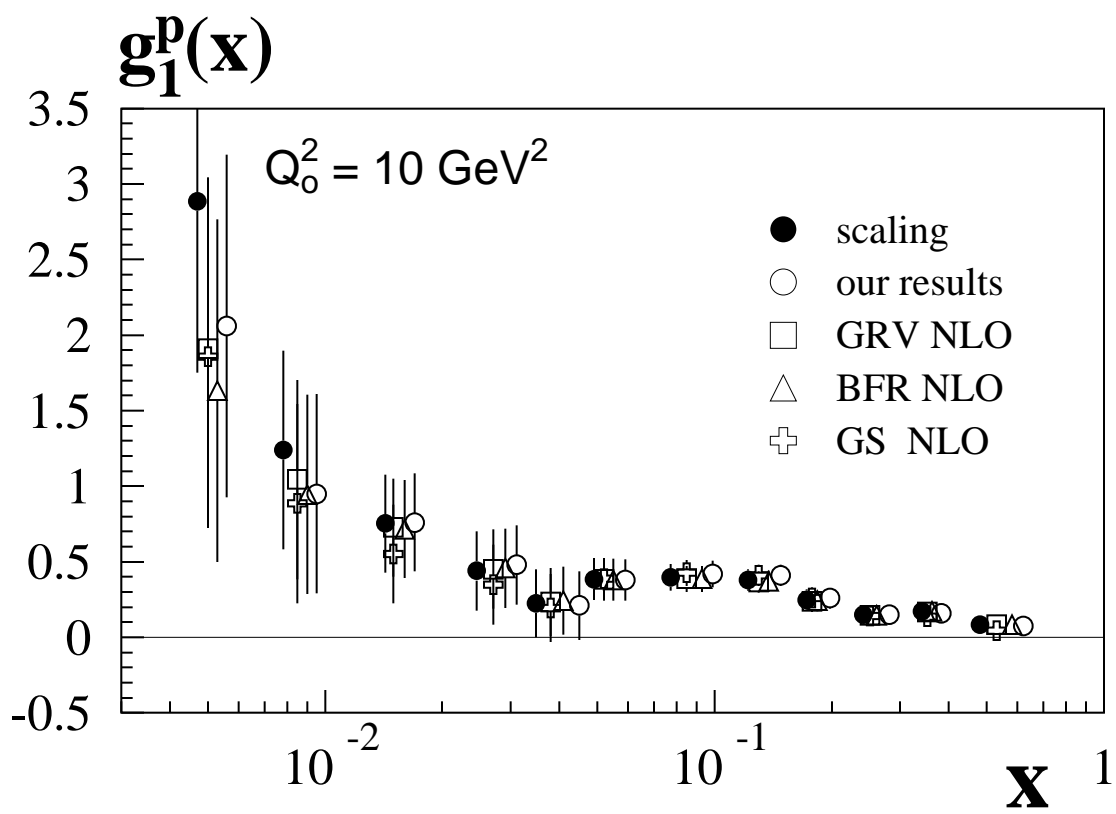
Table 2. The values of the coefficients of CCFR data parametrization.

Q^2 (GeV ²)	100	30	10	5	3
SMC proton [2] and deuteron data [3]					
A_1 -scaling	0.247	0.226	0.202	0.186	0.170
A_1^* -scaling	0.210	0.201	0.191	0.184	0.176
Analysis of [2]			0.183	0.181 ± 0.035	
SMC proton [2] and E154 neutron data [6]					
A_1 -scaling	0.221	0.209	0.194	0.183	0.171
A_1^* -scaling	0.194	0.190	0.185	0.181	0.176
E143 proton and deuteron data [4]					
A_1 -scaling	0.170	0.169	0.165	0.160	0.154
A_1^* -scaling	0.163	0.162	0.160	0.157	0.154
Analysis of [4]				0.164 ± 0.021	0.164
E143 proton [4] and E154 neutron data [5, 6]					
A_1 -scaling	0.189	0.186	0.179	0.174	0.169
A_1^* -scaling	0.172	0.172	0.171	0.169	0.166
Analysis of [6]				0.171 ± 0.013	
Analysis of [4]				0.170 ± 0.012	
Theory	0.194	0.191	0.186	0.181 ± 0.002	0.177

Table 1. The values of $\Gamma_1^p - \Gamma_1^n$. The errors are shown only for several points for each set of data. Uncertainties of our analysis are comparable with ones of [2, 3, 4, 6].

Table 2. The values of the coefficients of CCFR data parametrization.

C_1	C_2	C_3	C_4	C_5	C_6
0.33092	3.5000	6.5739	-7.1015	2.5388	7.6944
C_7	C_8	C_9	C_{10}	C_{11}	
-8.4285	4.9135	-4.9857	-8.1629	1.8193	
B_1	B_2	B_3	B_4	B_5	B_6
-0.06101	3.5000	4.9728	-3.1309	-1.3361	0.94242
B_7	B_8	B_9	B_{10}	B_{11}	
0.11729	-0.92024	-1.6489	0.61776	0.38910	



$Q^2=5 \text{ GeV}^2$, E154 data

